nature materials

LETTERS

PUBLISHED ONLINE: 26 FEBRUARY 2012 | DOI: 10.1038/NMAT3254

Reversible electrical switching of spin polarization in multiferroic tunnel junctions

D. Pantel, S. Goetze, D. Hesse and M. Alexe*

Spin-polarized transport in ferromagnetic tunnel junctions, characterized by tunnel magnetoresistance[1], has already been proven to have great potential for application in the field of spintronics[2] and in magnetic random access memories[3]. Until recently, in such a junction the insulating barrier played only a passive role, namely to facilitate electron tunnelling between the ferromagnetic electrodes. However, new possibilities emerged when ferroelectric materials were used for the insulating barrier, as these possess a permanent dielectric polarization switchable between two stable states[4–9]. Adding to the two different magnetization alignments of the electrode, four non-volatile states are therefore possible in such multiferroic tunnel junctions[10,11]. Here, we show that owing to the coupling between magnetization and ferroelectric polarization at the interface between the electrode and barrier of a multiferroic tunnel junction, the spin polarization of the tunnelling electrons can be reversibly and remanently inverted by switching the ferroelectric polarization of the barrier. Selecting the spin direction of the tunnelling electrons by short electric pulses in the nanosecond range rather than by an applied magnetic field enables new possibilities for spin control in spintronic devices[12].

In a spintronic device the spin degree of freedom of an electron is used as well as its charge[2]. In a magnetic memory cell, such as magnetic random access memories (MRAM), the spin degree of freedom is usually controlled using local magnetic fields delivered by high currents. However, this approach is energetically unfavourable, and manipulating remanently the spin by short electric field pulses instead of large current pulses would be a great advantage[6,12]. As mentioned, a multiferroic tunnel junction (MFTJ) can exhibit four states, characterized by the tunnel magnetoresistance (TMR), which is determined by the spin polarization of the tunnelling electrons, and by the tunnel electroresistance (TER), given by different junction resistances for the two different ferroelectric polarization directions[4]. A combination of both TMR and TER is thus used to read the four above-mentioned states and to detect magnetoelectric effects, respectively the interplay between the ferroelectric polarization and magnetic properties at the multiferroic interfaces.

For the present study we have used multiferroic Co/$PbZr_{0.2}Ti_{0.8}O_3$/$La_{0.7}Sr_{0.3}MnO_3$ (Co/PZT/LSMO) tunnel junctions, epitaxially grown on (100)-oriented $SrTiO_3$ (STO) crystals (see Methods). Here, half-metallic LSMO with a nominal spin polarization of +100% (ref. 13) serves as an analyser for the spin polarization of the tunnelling electrons[6,14]. However, the spin polarizations of LSMO surfaces extracted from transport measurements usually yield less than +95% (ref. 15). PZT is a ferroelectric material with a very high spontaneous and remanent polarization ($P_S \approx 110\,\mu C\,cm^{-2}$ for thicker films[16]), which is advantageous for magnetoelectric coupling at a multiferroic interface by electronic means[17–19]. Whereas a large magnetoelectric effect is not expected at the LSMO/PZT interface because of the robust ferromagnetic properties of the LSMO in the composition used[6,20] the opposite applies to the Co/PZT interface.

The epitaxial and fully coherent growth of the oxide materials on the STO substrate is revealed by both high-resolution transmission electron microscopy (HRTEM) and atomic force microscopy (AFM) investigations. Figure 1a shows a HRTEM cross-section image of a typical tunnel junction with sharp interfaces. The high-quality, atomically smooth growth of the bottom LSMO electrode, necessary for high-quality tunnel junctions, is maintained even for relatively thick LSMO films (Fig. 1b). It is worth noting that the thickness of LSMO has to be large enough to maintain the effective resistance of the bottom electrode across the entire sample significantly lower than the tunnel resistance of any MFTJ device and to rule out any influence of the magnetoresistance of LSMO or of geometrical effects, as previously described[21]. PZT barrier layers with average thicknesses of about two to sixteen unit cells, respectively 1.0 nm to 6.4 nm, were coherently grown on the LSMO bottom electrode layers.

Piezoresponse force microscopy (PFM) investigations shown in Fig. 1c and d prove the ferroelectric character of the PZT layers down to at least 3.2 nm PZT layer thickness for a bare surface of PZT and in a MFTJ, respectively, at room temperature. The coercive voltage is about 1 V ($3\,MV\,cm^{-1}$), but it is well known that the ferroelectric coercive voltage increases for decreasing temperature. A single domain state of the as-grown PZT films with a ferroelectric polarization pointing away from the LSMO bottom electrode is also revealed by PFM. The overall electrical properties of the PZT and LSMO layers are similar to those obtained in ref. 16. The MFTJ is completed by thermal evaporation of about 20 nm metallic polycrystalline Co through a shadow mask. To protect the Co/PZT interface from possible oxidation, a 5 nm top Au layer was *in situ* deposited onto the Co electrode through the same mask.

It is worth noting that the present devices are large-area devices ($4{,}000\,\mu m^2$) and that they do not require extensive and expensive photolithography and/or processing. Despite this, the tunnelling properties are similar to those previously reported in the literature for nanoscale devices. The product of the MFTJ resistance and device area (RA) is greater than $10\,M\Omega\,\mu m^2$ for PZT barrier thicknesses larger than 1 nm (see Supplementary Fig. S1), consistent with the previous analysis of tunnel junctions[22] and with data for MFTJs (refs 6,7) and Co/STO/LSMO junctions[14,23]. This, along with the analysis of the tunnel current in the Brinkman model[24], shown in Supplementary Fig. S1, supports the fact that even in large-area devices tunnelling is the dominant transport mechanism, provided

Max Planck Institute of Microstructure Physics, Weinberg 2, 06120 Halle (Saale), Germany. *e-mail: malexe@mpi-halle.de.

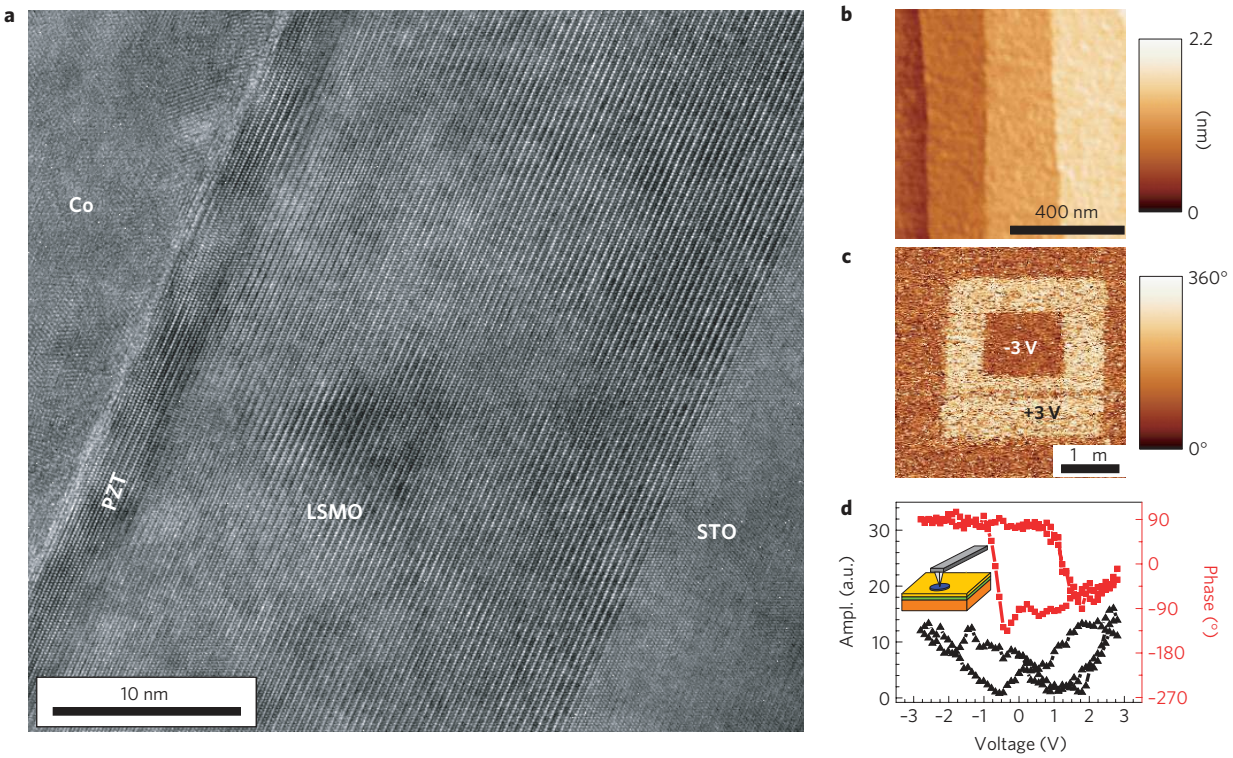

Figure 1 | Structure and basic properties of the multiferroic tunnel junctions. a, HRTEM image of a Co/PZT/LSMO tunnel junction; the PZT and LSMO layers are 3.2 nm and 32 nm thick, respectively. **b**, AFM-topography image of a 50 nm thick LSMO layer, showing the atomically smooth surface, preserving the terraces of the vicinal STO substrate. **c**, Piezoresponse (phase) measured after successively switching the polarization of a 3.2 nm PZT layer without Co top electrode with +3 V and −3 V. **d**, PFM amplitude (red squares) and phase (black triangles) on a MFTJ (as depicted in the inset) proving the ferroelectric nature of the PZT layer sandwiched between the Co and LSMO.

a high-quality barrier is used. Indeed, the properties, for example the temperature and voltage dependencies of the TMR, and the resistance of the Co/PZT/LSMO tunnel junctions are similar to those found in Co/STO/LSMO tunnel junctions[14], as shown in Supplementary Fig. S2, albeit here some properties can be modified by the ferroelectric polarization.

The values of the TMR, which are lower than the theoretical values expected in the Jullière model[1] from the spin polarization values of LSMO and Co, can be improved by a smaller junction size, reducing the probability of defects within the barrier and therefore of spin-independent transport channels. Furthermore, different terminations of the LSMO, different interface structures at the PZT/Co interface underneath the large area Co-electrodes, or a magnetic multi-domain structure of the electrodes may have reduced the TMR.

The Co/PZT/LSMO tunnel junctions should in principle exhibit a TMR due to the ferromagnetic electrodes as well as a TER given by the switching of the ferroelectric polarization of the barrier, as explained above. However, if the PZT is too thin the TER vanishes and if it is too thick it suppresses the TMR. These effects can be explained by a loss of ferroelectricity due to increasing depolarization fields[25] and by transport mechanisms different from direct tunnelling, respectively. But, as shown in Fig. 2a, a MFTJ with an intermediate PZT thickness of 3.2 nm exhibits a TMR at 50 K, and the resistance can be switched from low (ON state, 5.6 kΩ) to high (OFF state, 62 kΩ) and vice versa (Fig. 2b) if the polarization is switched from pointing towards Co to pointing towards LSMO by an electric field. TMR data for the other PZT barrier thicknesses are shown in Supplementary Fig. S3.

For similar heterostructures we recently showed that the resistive switching is due to ferroelectric polarization reversal, both occurring at the same electric field[16]. As resistive switching occurs here at a similar electric field range (however at slightly higher fields, due to the known thickness dependence of the ferroelectric coercive field[26]), it is reasonable to assume that the observed resistive switching has a purely electronic and not a electrochemical origin[27].

Surprisingly, switching the polarization from pointing towards Co (the as-grown state) to pointing towards LSMO, by applying a +3 V external voltage pulse to the Co electrode, not only modifies the resistance of the junction, but also switches the TMR from inverse (−3% at 50 K) to normal (+4%, see Fig. 2a). Moreover, by switching the ferroelectric polarization back with a −3 V pulse, the TMR switches back to its initial inverse sign. Subsequent voltage pulses, as shown in Fig. 2b and Supplementary Fig. S4, switch the TMR accordingly. Figure 2b summarizes the combined TER and TMR effect at 10 K as the polarization switches from one state to the other under the application of 3 V voltage pulses. The MFTJ resistance switches reversibly from about 11 kΩ to about 70 kΩ, while simultaneously the TMR changes from about −7.5% to +5%. The switching time between the two TMR states is chiefly determined by the switching time of the ferroelectric polarization. In the present case, the shortest voltage pulse which still switched the polarization was as short as 250 ns. The effect was observed over a wide temperature range up to about 250 K (Fig. 2c), the only limitation being the ferromagnetic properties of the bottom LSMO layer[12].

The performance of the devices could be extended to well above room temperature by using a half-metallic material with a higher Curie temperature as the bottom electrode. However, the choice of bottom electrode materials is restricted by the prerequisite of being chemically and structurally compatible with the ferroelectric PZT barrier. Possible candidates are the half-metallic double perovskites[28].

Figure 2d shows that, besides the two non-volatile TER states, the two magnetic states are truly non-volatile. These results not

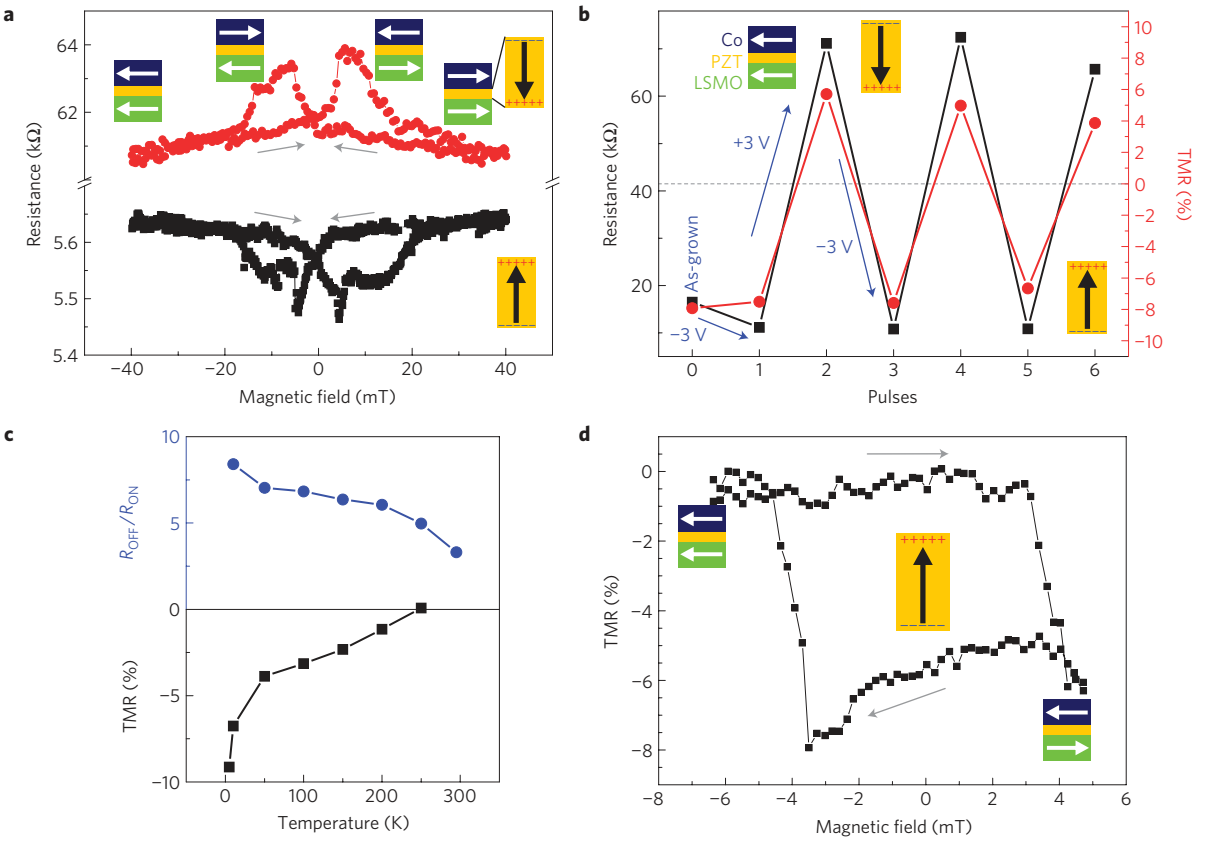

Figure 2 | Tunnel electro- and magnetoresistance properties of Co/PZT(3.2 nm)/LSMO junctions. a, Resistance versus magnetic field curves measured at 50 K in the as-grown state of a junction (black squares) and after polarization switching with a +3 V applied electrical bias (red circles). The polarization state of the barrier as well as magnetization directions in each magnetic layer are schematically shown for each non-volatile state. **b**, Resistance (black squares) and TMR (red circles) after successive switching with ±3 V voltage pulses for a different junction at 10 K. The first data point shows the respective value in the as-grown state. The minimum voltage pulse width required to switch the TMR from the inverse to normal state is 250 ns. **c**, Temperature dependence of the TMR (black squares) and of the TER, given as resistance ratio between OFF and ON (blue circles). **d**, TMR versus magnetic field (minor loop) in the as-grown state of the junction in **c** after electrode magnetizations were aligned parallel with an applied magnetic field of −100 mT at 10 K.

only show that a MFTJ is a four-state non-volatile memory cell, as shown theoretically[11,17,19] and experimentally[6,7,9] before, but also, in contrast to earlier experiments, that switching the ferroelectric polarization inverts the spin polarization at the Co/PZT interface. We assume that this is due to the polarization being higher in our ferroelectric PZT barrier than in the commonly used $BaTiO_3$ barriers[6,9] or due to a difference in the interface between Co/PZT and Co/$BaTiO_3$.

The spin inversion is in some ways similar to that described by De Teresa *et al.*[14] in Co/STO/LSMO tunnel junctions, where the sign of the spin polarization at a Co/STO interface, and thus the sign of the TMR of the junction, can be changed (albeit permanently) by inserting an additional Al_2O_3 layer between Co and STO. However, in our case the ferroelectric polarization of the PZT layer switches the spin polarization, and consequently the TMR, in a fully reversible as well as remanent way between positive and negative TMR. Therefore, the spin direction of carriers injected into, for example, a spin-based device can be selected without any applied magnetic field, just by the ferroelectric polarization direction. Because the ferroelectric polarization is controlled by short voltage pulses, this is a fast and energy-saving way of controlling the spin polarization and a major advantage over previously achieved changes in the spin polarization by low voltage pulses.

The microscopic mechanism of this effect is most probably an electronic effect given by a strong magnetoelectric coupling between the ferroelectric polarization and magnetization at one of the two multiferroic interfaces[11,17]. As such an effect is not expected at the PZT/LSMO interface with our composition of LSMO (refs 6,20), the change in spin polarization and the magnetoelectric effect is most probably located at the Co/PZT interface. The magnetoelectric coupling at such a multiferroic interface could be due to hybridization at the interface, charge-carrier doping, or spin-dependent screening in the magnetic electrode[29], as discussed below.

The hybridization effect within the first interface layers was investigated in *ab initio* studies by Fechner *et al.*[18,30] and was recently experimentally demonstrated for Co or iron (Fe) on top of ferroelectric $BaTiO_3$ (ref. 9). The theoretical studies revealed that for Fe on top of $PbTiO_3$, a system which is quite similar to the Co/PZT interface investigated here, the magnetic moment of the interfacial Ti ion changes drastically with ferroelectric polarization direction[18]. For the polarization pointing towards the interface (Fe) the magnetic moment of the Ti is aligned antiparallel to the Fe magnetic moment, owing to the hybridization between Fe and Ti, whereas for the other polarization direction almost no magnetic moment is induced on Ti (ref. 18). This can be explained on the basis of the distance between the Fe and Ti atoms. We assume the same situation for the Co/PZT interface as sketched in Fig. 3. A similar interface structure was found to be energetically favourable for the Co/STO interface (an interface similar to the Co/PZT interface[31]). The real structure at the Co/PZT interface might be different, either because of oxygen located at the interface, as is the case for Fe on $BaTiO_3$ (ref. 32), or because of the polycrystalline nature of the cobalt. Nevertheless, the magnetic moment at the

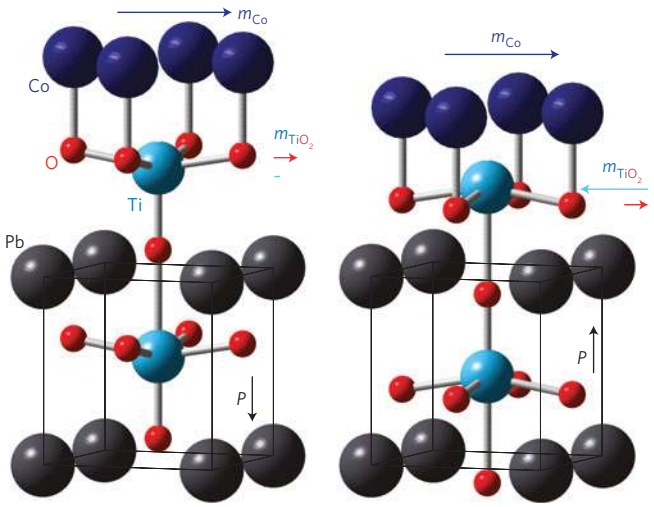

Figure 3 | Model of the influence of the ferroelectric polarization on the spin polarization. A microscopic model of the Co/PZT interface similar to refs 18,30, which reveals the reversal of spin polarization at the interface by switching of the ferroelectric polarization *P*. The model is based on the different bonding lengths (and strengths) between Ti and Co for different polarization directions. The induced local magnetic moment m_{Ti} on the interfacial Ti ion is antiparallel (almost 0) to the Co magnetization m_{Co} for polarization pointing towards Co (towards LSMO, as shown in the left image).

interface can still be changed by polarization direction even if oxygen is present at the interface[18].

It was shown that the negative spin polarization at the Co/STO interface observed in Co/STO/LSMO tunnel junctions is due to the induced magnetic moment on the interfacial Ti, which is aligned antiparallel to the Co magnetic moment[31]. Analogously, the sign of the spin polarization at our Co/PZT interface is negative if the polarization points towards Co. For the polarization pointing towards LSMO the antiparallel magnetic moment on the Ti vanishes and the spin polarization at the interface is positive. This should lead to inverse or normal TMR for the polarization pointing towards or away from the Co electrode, respectively.

A second possible explanation relies on the basic concept of spin-dependent screening due to splitting of the conduction band in the ferromagnetic electrodes into majority and minority spin bands because of exchange splitting[33]. In the case of half-metallic LSMO, the Fermi energy lies in the resulting energy gap, leading to a fully spin-polarized conduction band. The polarization switching changes the potential energy landscape as a result of an electrostatic contribution due to unscreened polarization charges[17]. It has been theoretically calculated that this can lead to a change in the sign of the TMR if one electrode is half-metallic, as is the case here[19].

Both the above-described models can equally explain the experimentally observed behaviour of the present Co/PZT/LSMO tunnel junctions. Nonetheless, inversion of the sign of the TMR could also possibly be induced by other effects, such as resonant tunnelling[34] or electrochemical effects[35], but we believe that this is not the case here. A contribution from resonant tunnelling can be ruled out because different defect levels in the barrier are averaged out over the large junction size[34]. Electrochemical effects rely on the segregation and oxidation of another metal at the barrier/electrode interface[35], for example Cr, which is not present in our junctions. Furthermore, in the absence of ferroelectricity, for instance for a barrier thickness of 1 nm, the junctions do not show a switchable TMR or TER (see Supplementary Fig. S4) as in the case of Co/STO/LSMO junctions[14,35].

The effect presented shows that polarization plays an important role in the electronic and magnetic reconstruction of multiferroic interfaces and in determining the spin polarization in MFTJs, that is, polarization switching fundamentally influences the magnetic ground state of the ferroelectric–ferromagnetic multiferroic interfaces. This has important implications for both the understanding of the origin of spin-polarized transport at multiferroic interfaces and for applications. Showing clearly the ability to control the amount and sign of the spin polarization by using small voltages in macroscopically large tunnel junctions paves the way for both four-state memory devices and spintronics.

Methods

Sample preparation. The oxide films were epitaxially grown by pulsed laser deposition on (100)-oriented STO substrates at temperatures between 550 °C and 600 °C in an oxygen atmosphere of 0.2 mbar by ablating stoichiometric ceramic targets (with 10% Pb excess for the PZT target). The 0.1° off-cut STO (100)-oriented substrates were etched and annealed before deposition to obtain an atomically flat, single TiO_2-terminated surface. The energy fluence of the KrF excimer laser ($\lambda = 248$ nm) at the target was about 300 mJ cm^{-2}. The ferromagnetic top Co electrodes (4,000 μm^2) were prepared by thermal evaporation from a tungsten coil through a shadow mask and subsequently capped by a protective Au layer. The pressure during the room-temperature deposition process was kept below 7×10^{-6} mbar to prevent oxidation of the Co layer.

Structural characterization. The oxide heterostructures are grown epitaxially and fully strained on the STO substrate, as shown by HRTEM and X-ray diffraction (Philipps X'Pert MRD), with a quality similar to ref. 16. HRTEM investigations were performed using a JEM-4010. HRTEM samples were prepared by mechanical and focused ion-beam milling.

Electrical characterization. The ferroelectricity of the ultrathin PZT layers was confirmed by PFM. These AFM-based investigations were carried out using a XE-100 AFM (Park Systems) with a conductive AFM tip (NSC35/Pt) in contact mode. An a.c. probing voltage ($f = 24.5$ kHz) with an amplitude of 0.5 V (below the effective coercive voltage of the PZT films) was applied to the tip. A lock-in amplifier (SR 830 DSP) was used to detect the piezoresponse signal. For remanent hysteresis measurements a poling voltage pulse (200 ms) was applied to the tip to switch the polarization. Afterwards, the PFM signal was measured. The poling voltage was varied between ±3 V.

Temperature-dependent magnetoresistance measurements were performed using a low-temperature probe station equipped with a superconducting solenoid (LakeShore CPX-HF). The measurements were performed in two-probe geometry with a Keithley Sourcemeter 2635 in constant voltage mode (10 mV). The resistance of the bottom electrode was estimated from the LSMO resistivity (about 30 Ω at 10 K) to be well below the junction resistance, therefore not influencing the measurement. The ferroelectric polarization was switched by rectangular voltage pulses (3 V) applied to the top Co electrode and generated by an arbitrary function generator. The TMR is defined as:

$$\mathrm{TMR} = \frac{R_{\mathrm{antiparallel}} - R_{\mathrm{parallel}}}{R_{\mathrm{antiparallel}}}$$

where $R_{\mathrm{antiparallel}}$ is the junction resistance in the antiparallel magnetic state and R_{parallel} is the resistance in the parallel magnetic state.

Received 27 October 2011; accepted 25 January 2012; published online 26 February 2012

References

1. Jullière, M. Tunneling between ferromagnetic films. *Phys. Lett. A* **54,** 225–226 (1975).
2. Wolf, S. A. *et al.* Spintronics: A spin-based electronics vision for the future. *Science* **294,** 1488–1495 (2001).
3. Slaughter, J. M. Materials for magnetoresistive random access memory. *Annu. Rev. Mater. Res.* **39,** 277–296 (2009).
4. Tsymbal, E. Y. & Kohlstedt, H. Tunneling across a ferroelectric. *Science* **313,** 181–183 (2006).
5. Gajek, M. *et al.* Tunnel junctions with multiferroic barriers. *Nature Mater.* **6,** 296–302 (2007).
6. Garcia, V. *et al.* Ferroelectric control of spin polarization. *Science* **327,** 1106–1110 (2010).
7. Hambe, M. *et al.* Crossing an interface: Ferroelectric control of tunnel currents in magnetic complex oxide heterostructures. *Adv. Funct. Mater.* **20,** 2436–2441 (2010).
8. Yin, Y. W. *et al.* Coexistence of tunneling magnetoresistance and electroresistance at room temperature in $La_{0.7}Sr_{0.3}MnO_3$/(Ba,Sr)TiO_3/$La_{0.7}Sr_{0.3}MnO_3$ multiferroic tunnel junctions. *J. Appl. Phys.* **109,** 07D915 (2011).

9. Valencia, S. *et al.* Interface-induced room-temperature multiferroicity in $BaTiO_3$. *Nature Mater.* **10,** 753–758 (2011).
10. Scott, J. F. Data storage: Multiferroic memories. *Nature Mater.* **6,** 256–257 (2007).
11. Velev, J. P. *et al.* Magnetic tunnel junctions with ferroelectric barriers: Prediction of four resistance states from first principles. *Nano Lett.* **9,** 427–432 (2009).
12. Ramesh, R. Ferroelectrics: A new spin on spintronics. *Nature Mater.* **9,** 380–381 (2010).
13. Park, J-H. *et al.* Direct evidence for a half-metallic ferromagnet. *Nature* **392,** 794–796 (1998).
14. De Teresa, J. M. *et al.* Role of metal-oxide interface in determining the spin polarization of magnetic tunnel junctions. *Science* **286,** 507–509 (1999).
15. Bowen, M. *et al.* Nearly total spin polarization in $La_{2/3}Sr_{1/3}MnO_3$ from tunneling experiments. *Appl. Phys. Lett.* **82,** 233–235 (2003).
16. Pantel, D., Goetze, S., Hesse, D. & Alexe, M. Room temperature ferroelectric resistive switching in ultra-thin $Pb(Zr_{0.2}Ti_{0.8})O_3$ films. *ACS Nano* **5,** 6032–6038 (2011).
17. Zhuravlev, M. Y., Jaswal, S. S., Tsymbal, E. Y. & Sabirianov, R. F. Ferroelectric switch for spin injection. *Appl. Phys. Lett.* **87,** 222114 (2005).
18. Fechner, M., Ostanin, S. & Mertig, I. Effect of oxidation of the ultrathin Fe electrode material on the strength of magnetoelectric coupling in composite multiferroics. *Phys. Rev. B* **80,** 094405 (2009).
19. Zhuravlev, M. Y., Maekawa, S. & Tsymbal, E. Y. Effect of spin-dependent screening on tunneling electroresistance and tunneling magnetoresistance in multiferroic tunnel junctions. *Phys. Rev. B* **81,** 104419 (2010).
20. Burton, J. D. & Tsymbal, E. Y. Prediction of electrically induced magnetic reconstruction at the manganite/ferroelectric interface. *Phys. Rev. B* **80,** 174406 (2009).
21. Van de Veerdonk, R. J. M., Nowak, J., Meservey, R., Moodera, J. S. & de Jonge, W. J. M. Current distribution effects in magnetoresistive tunnel junctions. *Appl. Phys. Lett.* **71,** 2839–2841 (1997).
22. Åkerman, J. J., Slaughter, J. M., Dave, R. W. & Schuller, I. K. Tunneling criteria for magnetic-insulator-magnetic structures. *Appl. Phys. Lett.* **79,** 3104–3106 (2001).
23. Vera Marún, I. J., Postma, F. M., Lodder, J. C. & Jansen, R. Tunneling magnetoresistance with positive and negative sign in $La_{0.67}Sr_{0.33}MnO_3/SrTiO_3/Co$ junctions. *Phys. Rev. B* **76,** 064426 (2007).
24. Brinkman, W. F., Dynes, R. C. & Rowell, J. M. Tunneling conductance of asymmetrical barriers. *J. Appl. Phys.* **41,** 1915–1921 (1970).
25. Junquera, J. & Ghosez, P. Critical thickness for ferroelectricity in perovskite ultrathin films. *Nature* **422,** 506–509 (2003).
26. Kay, H. F. & Dunn, J. W. Thickness dependence of the nucleation field of triglycine sulphate. *Phil. Mag.* **7,** 2027–2034 (1962).
27. Kalinin, S., Jesse, S., Tselev, A., Baddorf, A. P. & Balke, N. The role of electrochemical phenomena in scanning probe microscopy of ferroelectric thin films. *ACS Nano* **5,** 5683–5691 (2011).
28. Kobayashi, K-I., Kimura, T., Sawada, H., Terakura, K. & Tokura, Y. Room-temperature magnetoresistance in an oxide material with an ordered double-perovskite structure. *Nature* **395,** 677–680 (1998).
29. Velev, J. P., Jaswal, S. S. & Tsymbal, E. Y. Multi-ferroic and magnetoelectric materials and interfaces. *Phil. Trans. R. Soc. A* **369,** 3069–3097 (2011).
30. Fechner, M. *et al.* Magnetic phase transition in two-phase multiferroics predicted from first principles. *Phys. Rev. B* **78,** 212406 (2008).
31. Oleinik, I. I., Tsymbal, E. Y. & Pettifor, D. G. Atomic and electronic structure of $Co/SrTiO_3/Co$ magnetic tunnel junctions. *Phys. Rev. B* **65,** 020401 (2001).
32. Bocher, L. *et al.* Atomic and electronic structure of the $BaTiO_3/Fe$ interface in multiferroic tunnel junctions. *Nano Lett.* **12,** 376–378 (2012).
33. Zhang, S. Spin-dependent surface screening in ferromagnets and magnetic tunnel junctions. *Phys. Rev. Lett.* **83,** 640–643 (1999).
34. Tsymbal, E. Y., Sokolov, A., Sabirianov, I. F. & Doudin, B. Resonant inversion of tunneling magnetoresistance. *Phys. Rev. Lett.* **90,** 186602 (2003).
35. Bowen, M. *et al.* Bias-crafted magnetic tunnel junctions with bistable spin-dependent states. *Appl. Phys. Lett.* **89,** 103517 (2006).

Acknowledgements

This work has been supported by the German Science Foundation (DFG) through SFB 762. We are grateful to N. Schammelt for technical assistance and G. Schmidt for useful discussions. We thank P. Werner for help with HRTEM.

Author contributions

D.P. and M.A. designed the experiments; D.P. carried out the experiments; S.G. and D.P. prepared the samples; S.G. carried out the TEM investigations; D.P. and M.A. analysed and discussed the results; D.P., M.A. and D.H. prepared the manuscript.

Additional information

The authors declare no competing financial interests. Supplementary information accompanies this paper on www.nature.com/naturematerials. Reprints and permissions information is available online at www.nature.com/reprints. Correspondence and requests for materials should be addressed to M.A.

nature materials

SUPPLEMENTARY INFORMATION

DOI: 10.1038/NMAT3254

Reversible electrical switching of spin polarization in multiferroic tunnel junctions

D. Pantel, S. Goetze, D. Hesse, M. Alexe

Max Planck Institute of Microstructure Physics, Weinberg 2, 06120 Halle (Saale), Germany

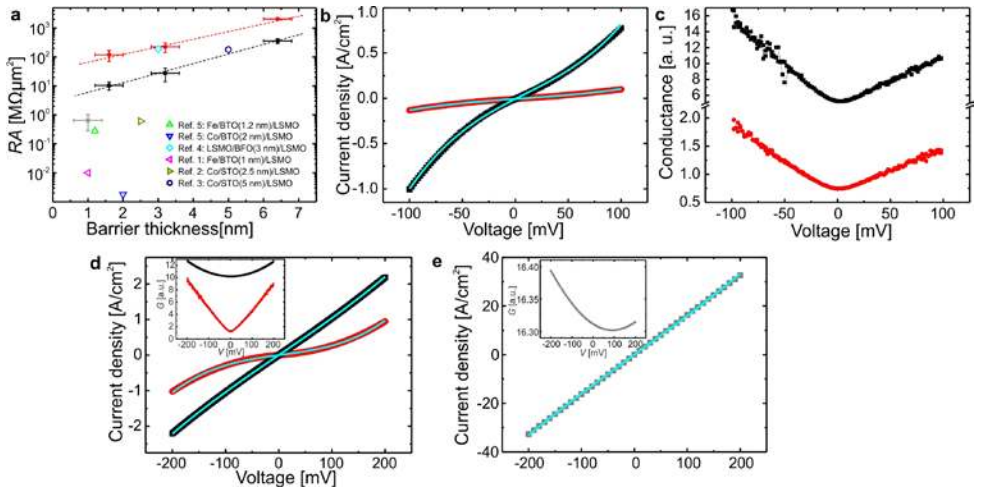

Figure S1. Tunneling properties of the MFTJs. a Resistance area product *RA* versus barrier thickness of Co/PZT/LSMO junctions and tunnel junctions from the literature [1, 2, 3, 4, 5] at 10 K. The tunnel junction with a barrier thickness of 1 nm (■) does not show ferroelectricity and hence no electroresistance. **b** Current density *j* and **c** tunneling conductance *G* ($G = \mathrm{d}j/\mathrm{d}V$) of a Co/PZT(3.2nm)/LSMO junction as a function of voltage *V* at 50 K. Current density as a function of voltage for a MFTJ with a **d** 1.6 nm and **e** 1.0 nm thick PZT barrier. The insets show $\mathrm{d}j/\mathrm{d}V$ versus *V*. The solid lines in **b, d**, and **e** represent a fit according to the Brinkman model [6]. In subfigures **a-d**, the ferroelectric ON-state (OFF-state) is represented by -■- (-●-).

The *RA* product in the Co/PZT/LSMO is in the range (or above) the values of similar tunnel junctions reported in the literature [1, 2, 3, 4, 5]. Furthermore, the resistance (and hence the *RA* product) exponentially depends on PZT-barrier thickness, which is expected for tunneling. The tunneling conductance shows a parabola-like dependence on voltage and the *j*(*V*)-curves fit with the Brinkman model [6]. The Brinkman model describes direct tunneling of charge carriers with an effective tunneling mass $m_{e,ox}$ through a metal/insulator/metal junction. The potential energy barrier is characterized by thickness *d* of the insulator and the potential energy barrier height Φ_1 and Φ_2 at the metal/insulator interfaces. The extracted parameters are given in Tab. S1. The barrier thickness *d* agrees well with the measured

DOI: 10.1038/NMAT3254

thickness. The effective tunneling mass $m_{e,ox}$ is in agreement with literature values for ferroelectric barriers (1 to 6 m_e [7, 8, 1, 9]). Barrier heights $\Phi_{1/2}$, are in the range of usual values for PZT electrode interfaces (0.6 to 1.3 eV, see, e.g., Ref.[10, 11, 12]). Especially for the 3.2 nm thick PZT barrier values are slightly lower. Therefore, other contributions to the transport in these large area (4000 μm^2) junctions cannot be excluded, but should not be dominant, and thus the direct tunneling should govern the transport in the Co/PZT(3.2 nm)/LSMO junctions.

Table S1: Parameter extracted from the IV curves in Fig. S1 by fitting to the Brinkman model.

Fig.	Ferroelectric state	d	$m_{e,ox}$	Φ_1	Φ_2
S1b	OFF	3.2 nm	1.2 m_e	0.20 eV	0.44 eV
S1b	ON	3.2 nm	1.2 m_e	0.13 eV	0.39 eV
S1d	OFF	1.6 nm	4.7 m_e	0.28 eV	0.42 eV
S1d	ON	1.6 nm	1.0 m_e	1.35 eV	1.41 eV
S1e	-	0.9 nm	2.5 m_e	1.62 eV	1.63 eV

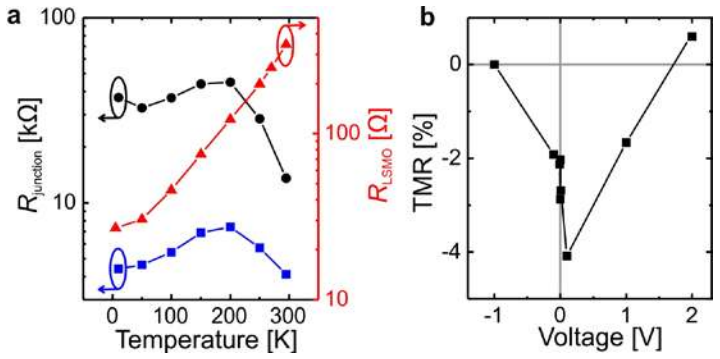

Figure S2. Temperature and voltage dependency. a Temperature dependence of the resistance $R_{junction}$ of a Co/PZT(3.2nm)/LSMO junction with parallel magnetizations and polarization pointing towards Co and LSMO (-■- and -●-), respectively, and the estimated serial resistance of the LSMO bottom electrode R_{LSMO} (-▲-). **b** Voltage dependence of the TMR of a junction for polarization towards Co at 50 K. The lines are guide to the eye.

The serial resistance of the LSMO bottom electrode is almost two orders of magnitude lower than the junction resistance at all investigated temperatures. Hence, it cannot contribute to the observed magneto- and electroresistive behavior. The junction resistance increases slightly with increasing temperature from 10 K to about 200 K. At higher temperatures it decreases with increasing temperature. The overall resistance change from 10 K to 300 K is less than a factor of 3. This is the temperature dependency of the resistance which is commonly observed for high quality LSMO-based tunnel junctions [3, 1, 13]. This behavior is in contrast to oxygen deficient or defective barriers which yield strong temperature dependence [3].

The TMR decreases as the negative bias voltage increases. It has a maximum at positive bias (≈100 mV) and at large positive voltages it becomes positive. This is a similar behavior as in the Co/STO/LSMO system and reveals that the tunneling for polarization towards Co is predominantly due to the *d*-character electrons [2].

Together with Fig. 2d from the main manuscript showing the temperature dependence of the TMR, these results confirm a similar quality of the tunnel junctions as usually observed for tunnel junctions with LSMO and Co electrodes separated by an epitaxial barrier.

DOI: 10.1038/NMAT3254

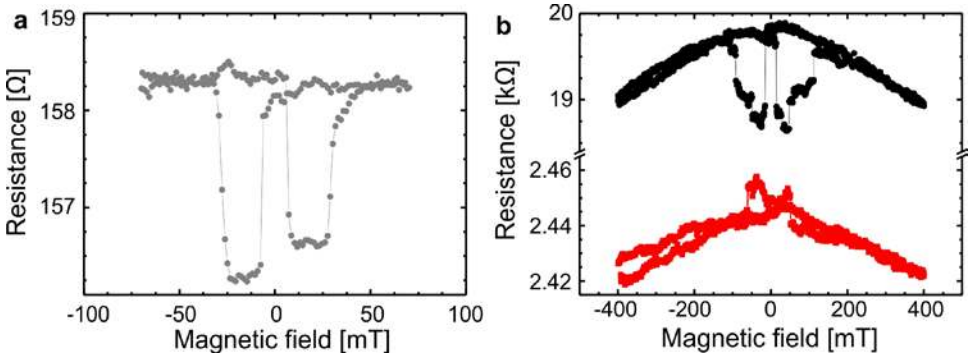

Figure S3. TMR for other PZT thicknesses. Magnetic field dependence of the resistance of a Co/PZT/LSMO junction with a PZT thickness of **a** 1.0 nm and **b** 1.6 nm at 50 K. The two measurements of **b** are from two different junctions in which the polarization state is pinned into opposite directions due to the small ferroelectric thickness.

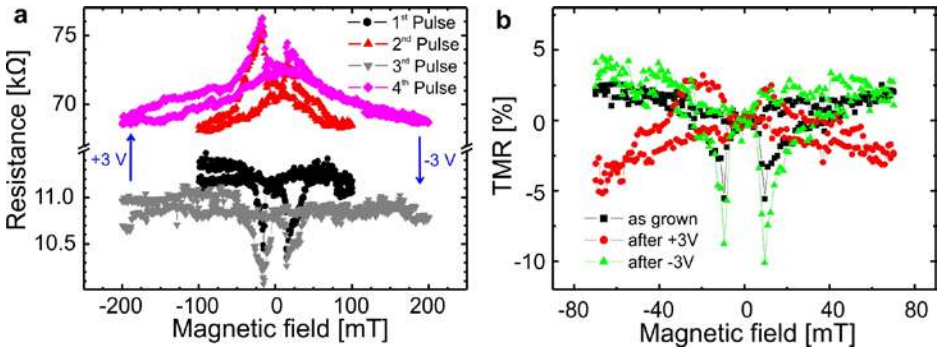

Figure S4. Switchable TMR. Magnetic field dependence of **a** the resistance and **b** the TMR of Co/PZT(3.2nm)/LSMO junctions at 10 K after voltage pulses of ±3 V applied to the Co electrode. **a** shows part of the raw data of Fig. 2b of the main manuscript and **b** data from another junction.

References:

[1] Garcia, V., Bibes, M., Bocher, L., Valencia, S., Kronast, F. *et al.*, Ferroelectric control of spin polarization. *Science* 327, 1106–1110 (2010).

[2] De Teresa, J. M., Barthélémy, A., Fert, A., Contour, J. P., Montaigne, F. *et al.*, Role of metal-oxide interface in determining the spin polarization of magnetic tunnel junctions. *Science* 286, 507–509 (1999).

[3] Vera Marún, I. J., Postma, F. M., Lodder, J. C. & Jansen, R., Tunneling magnetoresistance with positive and negative sign in $La_{0.67}Sr_{0.33}MnO_3/SrTiO_3/Co$ junctions. *Phys. Rev. B* 76, 064426 (2007).

[4] Hambe, M., Petraru, A., Pertsev, N. A., Munroe, P., Nagarajan, V. *et al.*, Crossing an interface: Ferroelectric control of tunnel currents in magnetic complex oxide heterostructures. *Adv. Funct. Mater.* 20, 2436–2441 (2010).

[5] Valencia, S., Crassous, A., Bocher, L., Garcia, V., Moya, X. *et al.*, Interface-induced room-temperature multiferroicity in $BaTiO_3$. *Nat. Mater.* 10, 753–758 (2011).

[6] Brinkman, W. F., Dynes, R. C. & Rowell, J. M., Tunneling conductance of asymmetrical barriers. *J. Appl. Phys.* 41, 1915–1921 (1970).

[7] Scott, J. F., *Ferroelectric memories* (Springer, Berlin, 2000).

[8] Gruverman, A., Wu, D., Lu, H., Wang, Y., Jang, H. W. *et al.*, Tunneling electroresistance effect in ferroelectric tunnel junctions at the nanoscale. *Nano Lett.* 9, 3539–3543 (2009).

[9] Berglund, C. N. & Baer, W. S., Electron transport in single-domain, ferroelectric barium titanate. *Phys. Rev.* 157, 358–366 (1967).

[10] Pintilie, L., Vrejoiu, I., Hesse, D., LeRhun, G. & Alexe, M., Ferroelectric polarization-leakage current relation in high quality epitaxial $Pb(Zr,Ti)O_3$ films. *Phys. Rev. B* 75, 104103 (2007).

[11] Sudhama, C., Campbell, A. C., Maniar, P. D., Jones, R. E., Moazzami, R. *et al.*, A model for electrical conduction in metal-ferroelectric-metal thin-film capacitors. *J. Appl. Phys.* 75, 1014–1022 (1994).

[12] Pintilie, L., Boerasu, I., Gomes, M. J. M., Zhao, T., Ramesh, R. *et al.*, Metal-ferroelectric-metal structures with Schottky contacts. II. Analysis of the experimental current-voltage and capacitance-voltage characteristics of $Pb(Zr,Ti)O_3$ thin films. *J. Appl. Phys.* 98, 124104 (2005).

[13] Ishii, Y., Yamada, H., Sato, H., Akoh, H., Ogawa, Y. *et al.*, Improved tunneling magnetoresistance in interface engineered $(La,Sr)MnO_3$ junctions. *Appl. Phys. Lett.* 89, 042509 (2006).